



~~CONFIDENTIAL~~

NATIONAL ADVISORY COMMITTEE FOR AERONAUTICS

RESEARCH MEMORANDUM

for the

Bureau of Aeronautics, Department of the Navy

ENGINEERING DEPARTMENT LIBRARY  
CHANCE VUGHT  
CF-108  
STRATFORD-CONN

AN INVESTIGATION OF THE AERODYNAMIC CHARACTERISTICS OF AN  
0.08-SCALE MODEL OF THE CHANCE VUGHT XF7U-1 AIRPLANE  
IN THE LANGLEY HIGH-SPEED 7- BY 10-FOOT TUNNEL  
PART VI - ESTIMATED HIGH-SPEED FLYING QUALITIES

REPORT NO. NACA DE308

By Charles J. Donlan and Richard E. Kuhn

SUMMARY

An analysis of the estimated high-speed flying qualities of the Chance Vought XF7U-1 airplane in the Mach number range from 0.40 to 0.91 has been made, based on tests of an 0.08-scale model of this airplane in the Langley high-speed 7- by 10-foot wind tunnel.

The analysis indicates longitudinal control-position instability at transonic speeds, but the accompanying trim changes are not large. Control-position maneuvering stability, however, is present for all speeds. Longitudinal and lateral control appear adequate, but the damping of the short-period longitudinal and lateral oscillations at high altitudes is poor and may require artificial damping.

INTRODUCTION

At the request of the Bureau of Aeronautics, Department of the Navy, an investigation of the stability and control characteristics of an 0.08-scale model of the Chance Vought XF7U-1 airplane was conducted in the Langley high-speed 7- by 10-foot tunnel.

~~CONFIDENTIAL~~

This report contains the results of an analysis of the estimated flying qualities of the Chance Vought XF7U-1 airplane in the Mach number range from 0.40 to 0.91. The analysis is based on the data obtained from tests of an 0.08-scale model of this airplane in the Langley high-speed 7- by 10-foot tunnel (references 1 to 5). Inasmuch as data for the landing configuration were not obtained from this model, the present study has been restricted to an analysis of high-speed configuration (landing gear and auxiliary lift devices retracted) for wing loadings of 24 and 34 pounds per square foot at sea level and at an altitude of 40,000 feet. All computations are based on a center-of-gravity position of 17 percent of the mean geometric chord.

#### COEFFICIENTS AND SYMBOLS

The system of axes employed, together with an indication of the positive forces, moment, and angles, is presented in figure 1. Pertinent symbols used in this report are defined as follows:

$C_L$	lift coefficient (Lift/qS)
$C_D$	drag coefficient (Drag/qS)
$C_m$	pitching-moment coefficient (Pitching moment/qSc')
$C_l$	rolling-moment coefficient (Rolling moment/qSb)
$C_Y$	side-force coefficient (Side force/qS)
$C_n$	yawing-moment coefficient (Yawing moment/qSb)
q	free-stream dynamic pressure, pounds per square foot $\left(\frac{\rho V^2}{2}\right)$
S	wing area
$c'$	wing mean geometric chord (M.G.C.)
c	chord, parallel to plane of symmetry
$c_l$	chord, perpendicular to 0.25c line
b	wing span
V	air velocity, feet per second
p	rolling velocity, degrees per second or radians per second

- a speed of sound, feet per second
- M Mach number  $(V/a)$
- R Reynolds number  $\left(\frac{\rho V c'}{\mu}\right)$
- $\mu$  absolute viscosity, pound-seconds per square foot
- $\rho$  mass density of air, slugs per cubic foot
- $\alpha$  angle of attack, measured from X-axis to fuselage center line, degrees
- $\delta$  control deflection, measured on chord line parallel to the plane of symmetry, degrees
- $\psi$  angle of yaw, measured from X-axis to fuselage center line, degrees
- L/D lift-drag ratio  $(C_L/C_D)$
- W/S wing loading, pounds per square foot (Weight/S)

$$C_{m_\delta} = \frac{\partial C_m}{\partial \delta}$$

$$C_{L_\psi} = \frac{\partial C_L}{\partial \psi}$$

$$C_{n_\psi} = \frac{\partial C_n}{\partial \psi}$$

$$C_{Y_\psi} = \frac{\partial C_Y}{\partial \psi}$$

$$C_{L_p} = \frac{\partial C_L}{\partial \left(\frac{pb}{2V}\right)}$$

Subscript:

a aileron

#### AIRPLANE AND MODEL

The Chance Vought XF7U-1 airplane is a twin-jet-propelled fighter intended for naval shipboard operation. The physical characteristics of

the airplane and of the solid-steel 0.08-scale model constructed by the manufacturer are compared in table I, and a drawing of the airplane is presented in figure 2. The dimensions in figure 2 have been scaled from the model values and may vary slightly from those of the airplane being built. The model was tested on the sting-support system as shown in figure 3. The control surfaces on this airplane are referred to as ailerons by the manufacturer and are used for both longitudinal and lateral controls. The model ailerons were true-contour flaps with sealed gaps. The rudders were not simulated on the model. Air flow through the jet-intake ducts was permitted for all tests, and one of the exhaust parts (together with its mirror image) can be seen in figure 3.

A complete description of the model and of the testing technique employed is given in reference 1.

#### BASIS OF ANALYSIS

The most recent Army-Navy specification for satisfactory flying qualities (reference 6) has been used as a guide in the present analysis. However, inasmuch as the analysis is restricted to the high-speed configuration without regard to control forces (no model hinge-moment data were obtained), and because much of the interest centers about the behavior of the airplane at transonic speeds, no detailed step-by-step comparison with the specifications has been attempted.

The estimated characteristics of the aircraft at each Mach number are based upon the results of tunnel tests at the same Mach number but at the test Reynolds number indicated in figure 4. The full-scale Reynolds numbers corresponding to flight at sea level and at an altitude of 40,000 feet are also shown in figure 4. No attempt was made to account for Reynolds number effects in interpreting the results, but a few unpublished tests made with transition fixed at the leading edge of the model were in good agreement with the basic free-transition tests. The bulk of the model test data was obtained with free transition.

#### RESULTS AND DISCUSSION

##### Performance

Flight conditions.— The variations with Mach number of the lift coefficient required for level flight for the various wing loadings and altitudes considered in the analysis are given in figure 5 and the

corresponding angle-of-attack variation is given in figure 6. Figure 6 is useful for estimating the inclination of the principal axes of inertia for the different flight conditions. It will be observed that the angle of attack for level flight at sea level for the lighter wing loading becomes slightly negative at the highest Mach numbers. This condition, of course, is a result of the shift in angle of zero lift effected by the deflected aillavators required for balance.

Lift-drag ratios.— The variation of the untrimmed lift-drag ratios at the various Mach numbers as a function of the lift coefficient is presented in figure 7. It will be observed that the lift coefficient for maximum L/D is essentially independent of Mach number although the magnitude of the available L/D maximum drops rather rapidly above a Mach number of 0.80. The level-flight L/D values associated with the trimmed-flight conditions defined in figure 5 are presented in figure 8. The advantages to be gained by flying at high altitude are forcefully illustrated by this figure.

#### Longitudinal Stability and Control

Static longitudinal stability.— The static longitudinal stability of the airplane is presented in figure 9 in the form of the variation of the aillavator position required for trim with Mach number. Control-position instability is first manifested at a Mach number of 0.90 at sea level and at a Mach number of 0.85 at an altitude of 40,000 feet. The causes of the control-position instability exhibited above these Mach numbers are traceable to the rapid changes occurring in the basic untrimmed pitching-moment coefficient (reference 1) and to the rapid changes in control effectiveness (fig. 10). The resultant changes in trim, however, appear to be relatively gradual and of moderate magnitude, at least to a Mach number of 0.91, and may not be objectionable.

A rigorous evaluation of the neutral-point location  $\left(\frac{d\delta}{dM} = 0\right)$  at these supercritical Mach numbers would indeed indicate that the control-fixed neutral point moves well ahead of the center-of-gravity position. However, the utility of the neutral-point concept largely vanishes at supercritical speeds where irregular and rapid changes in trim occur. The desired information on static longitudinal stability appears to be most directly conveyed through charts like figure 9.

Maneuvering stability.— The rate of change of the pitching-moment coefficient with lift coefficient at a constant Mach number  $\left(\frac{\partial C_m}{\partial C_L}\right)_M$  is an extremely important parameter governing the response of the aircraft

to gusts and rapid control deflections or any maneuver that may be considered to take place at a constant speed. For tailless aircraft (which possess very little damping in pitch) the factor  $\left(\frac{\partial c_m}{\partial c_L}\right)_M$  very nearly

defines the stick-fixed "maneuver margin" - the distance, expressed as a fraction of the chord, that the center of gravity is ahead of the "maneuver point." (The maneuver point is the center-of-gravity position for which the rate of change of control deflection with normal acceleration vanishes.)

The variation of the maneuver-point location with Mach number is presented for several lift coefficients in figure 11. In general, it is evident that the maneuver point moves rearward at the supercritical Mach numbers, except for the condition with the speed brakes open. However, because of the nonlinearities involved in the evaluation of the maneuver point, its influence can be studied more conveniently in conjunction with the evaluation of the effectiveness of the longitudinal control.

Longitudinal-control effectiveness.- The amount of ailerator control required for various accelerated-flight conditions is presented in figure 12. For flight at sea level (figs. 12(a) and 12(b)) only about 1° of ailerator is required to produce a 6g acceleration at a Mach number of 0.85. The ailerator must always be moved in the desired direction, however, even at supercritical speeds, as would be expected from the maneuver-point movement previously discussed (fig. 11). The minimum degree of stick-position maneuvering stability that can be tolerated will depend on the associated stick-force gradient. A small stick-position gradient, however, may make it difficult to design the power boost system to supply an adequate force gradient and still keep the maximum control force for other conditions within the capabilities of the pilot. At altitude (figs. 12(c) and 12(d)) much larger control deflections are required for the accelerated-flight conditions which makes the design of the power boost system even more critical.

Dynamic stability.- The characteristics of the stick-fixed short-period longitudinal oscillation are presented in figures 13 to 16. The computations are based on the formulas of reference 7. While it is desirable that the short-period oscillation be damped to one-tenth amplitude in one cycle, it is obvious from figure 16 that this tailless design would not meet such a requirement at altitude. For the altitude case, it is seen that an oscillation of about 40 percent of the original amplitude still persists after one complete oscillation. At sea level, on the other hand, the damping of the oscillation appears to be adequate.

The damping characteristics have been evaluated for the control-fixed condition although the specifications are based upon free controls. With

the irreversible boost system contemplated for this airplane, however, the fixed-control characteristics will dictate the behavior of the aircraft.

### Lateral Stability and Control

Lateral-stability parameters.- Because of the absence of any rudder data from which trimmed yawed conditions could be evaluated, the directional and lateral stability will be adjudged from the stability parameters presented in figure 17. This figure was obtained from the data presented in references 2 and 5. In general, the data indicate adequate static lateral stability. It will be noted, however, that the speed brakes decrease the directional stability and produce a slight negative dihedral effect (negative  $C_{l\psi}$ ) at the highest Mach numbers.

Lateral control.- The lateral-control characteristics of the airplane are presented in figure 18 in the form of the variation with Mach number of the wing-tip helix angle  $\frac{pb}{2V}$  obtained with various total aileron deflections  $\Delta\delta_a$ . The helix angle was computed from the simple

relation  $\frac{pb}{2V} = -\frac{C_{l_a}}{C_{l_p}}$  by use of the aileron rolling-moment data  $C_{l_a}$  of reference 4. The damping coefficient was estimated by the method of reference 8. Some unpublished experimental  $C_{l_p}$  data indicate that for this wing plan form the theoretical values are in good agreement with experiment.

The rate of roll expressed in degrees per second is presented in figure 19. Aeroelastic distortion effects would undoubtedly decrease the rates of roll from those indicated in figure 19, but in any event the rates of roll should be extremely high. It will be noted that, as in the case of longitudinal control, lateral-control effectiveness begins to decrease rapidly at the highest Mach numbers.

It is evident from the extremely rapid rates of roll possible on this airplane that the limiting rate of roll will probably be conditioned by the pilot's ability to withstand the angular accelerations imposed.

Dynamic stability.- The characteristics of the control-fixed lateral oscillations have been evaluated by the method of reference 9 and are presented in figures 20 to 23.

It will be noted from figure 23 that the damping of the oscillation is marginal for the sea-level conditions and is definitely unsatisfactory for the altitude conditions according to the desired damping criterion set forth in reference 6. If subsequent flight tests prove unsatisfactory in regard to the damping characteristics, it may be desirable to introduce artificial damping into the system in the form of aileron control coupled to a gyro instrument sensitive to rolling velocity or rudder control coupled to a gyro instrument sensitive to yawing velocity.

A check on spiral stability was also made for the conditions stated in figure 20. It was found that spiral instability was present at a Mach number above 0.9, but the degree of spiral instability was so slight that the time required for the angle of bank to increase 10 percent was of the order of 1 minute at an altitude of 40,000 feet and 4 minutes at sea level.

An estimate of the dynamic stability with speed brakes open was also made at a Mach number of 0.9 for level flight at sea level with a wing loading of 24 pounds per square foot. It was found that the period and damping of the oscillation were similar to those found for the speed-brake-retracted configuration presented in figures 20 to 22. The negative dihedral effect associated with the speed-brake configuration (fig. 17) increased the rate of spiral divergence although 100 seconds was still required for the angle of bank to increase by 10 percent of the original displacement for the sea-level condition.

#### CONCLUSIONS

An analysis of the estimated flying qualities of the Chance Vought XF7U-1 airplane in the Mach number range from 0.40 to 0.91 indicates the following conclusions:

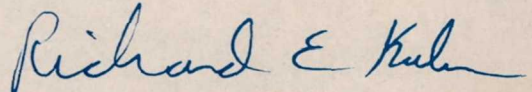
1. The airplane will exhibit longitudinal control-position instability at transonic speeds but the accompanying trim changes at these speeds will not be large.
2. Control-position maneuvering stability will be present at all speeds investigated although the control-position gradient may be as high as 6g's per degree of aileron deflection at low altitudes.
3. The damping of the short-period longitudinal oscillation at high altitudes will be less than desired.
4. The damping of the lateral oscillation at high altitude will be very poor and may require artificial damping.

5. Longitudinal and lateral control appear to be adequate at all speeds investigated.

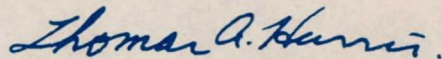
Langley Aeronautical Laboratory  
National Advisory Committee for Aeronautics  
Langley Field, Va.



Charles J. Donlan  
Aeronautical Research Scientist



Richard E. Kuhn  
Aeronautical Engineer



Approved:

Thomas A. Harris  
Chief of Stability Research Division

bpe

## REFERENCES

1. Kemp, William B., Jr., Kuhn, Richard E., and Goodson, Kenneth W.: An Investigation of the Aerodynamic Characteristics of an 0.08-Scale Model of the Chance Vought XF7U-1 Airplane in the Langley High-Speed 7- by 10-Foot Tunnel. Part I - Basic Longitudinal Stability Characteristics. TED No. NACA DE308. NACA RM No. L7G08, Bur. Aero., 1947.
2. Kemp, William B., Jr., Goodson, Kenneth W., and Kuhn, Richard E.: An Investigation of the Aerodynamic Characteristics of an 0.08-Scale Model of the Chance Vought XF7U-1 Airplane in the Langley High-Speed 7- by 10-Foot Tunnel. Part II - Basic Lateral Stability Characteristics - TED No. NACA DE308. NACA RM No. L7G10, Bur. Aero., 1947.
3. Kuhn, Richard E., and King, Thomas J., Jr.: An Investigation of the Aerodynamic Characteristics of an 0.08-Scale Model of the Chance Vought XF7U-1 Airplane in the Langley High-Speed 7- by 10-Foot Tunnel. Part III - Longitudinal Control Characteristics. TED No. NACA DE308. NACA RM No. L7H01, Bur. Aero., 1947.
4. Goodson, Kenneth W., and Myers, Boyd C., II: An Investigation of the Aerodynamic Characteristics of an 0.08-Scale Model of the Chance Vought XF7U-1 Airplane in the Langley High-Speed 7- by 10-Foot Tunnel. Part IV - Aileron Characteristics - TED No. NACA DE308. NACA RM No. L7H22, Bur. Aero., 1947.
5. Kuhn, Richard E., and Myers, Boyd C., II: An Investigation of the Aerodynamic Characteristics of an 0.08-Scale Model of the Chance Vought XF7U-1 Airplane in the Langley High-Speed 7- by 10-Foot Tunnel. Part V - Wing-Alone Tests and Effect of Modifications to the Vertical Fins, Speed Brakes, and Fuselage - TED No. NACA DE308. NACA RM No. L7J09, Bur. Aero., 1947.
6. Anon.: Specification for Flying Qualities of Piloted Airplanes. NAVAER SR-119B, Bur. Aero., June 1, 1948.
7. Greenburg, Harry, and Sternfield, Leonard: A Theoretical Investigation of Longitudinal Stability of Airplanes with Free Controls Including Effect of Friction in Control System. NACA Rep. No. 791, 1944.

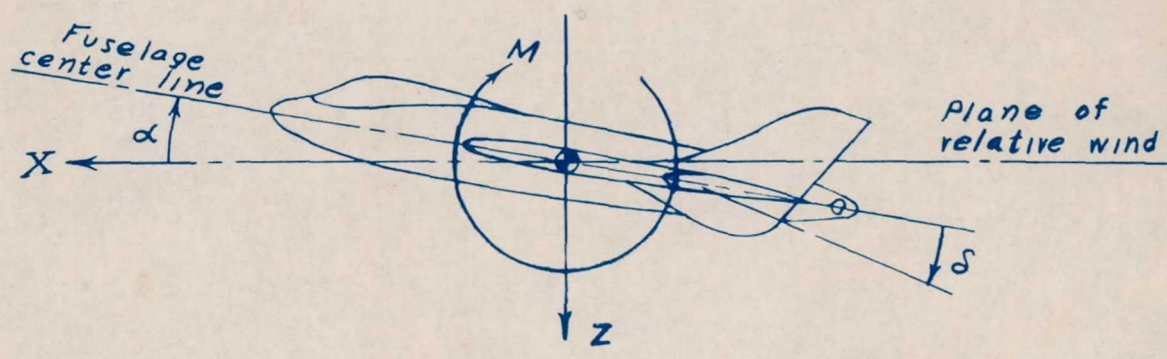
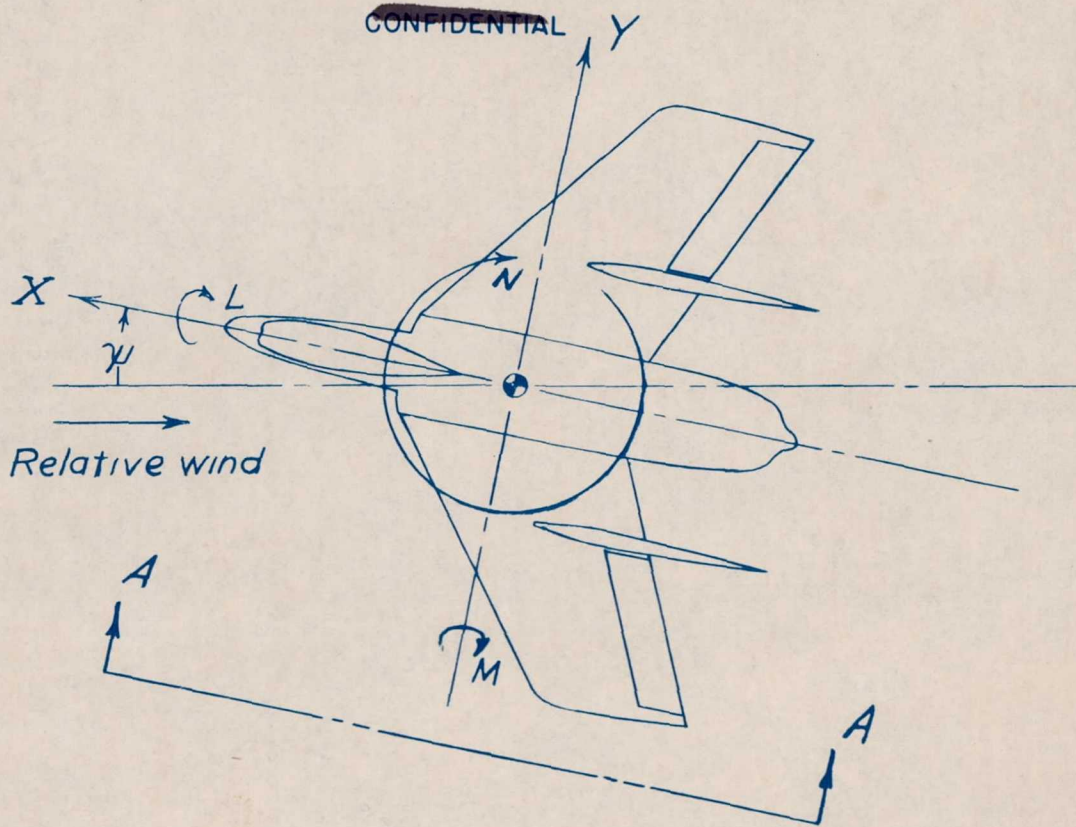
8. Swanson, Robert S., and Priddy, E. LaVerne: ~~Lifting-Surface-Theory~~ Values of the Damping in Roll and of the Parameter Used in Estimating Aileron Stick Forces. NACA ARR No. L5F23, 1945.
9. Sternfield, Leonard: Some Considerations of the Lateral Stability of High-Speed Aircraft. NACA TN No. 1282, 1947.

TABLE I

## PHYSICAL CHARACTERISTICS OF MODEL AND AIRPLANE

	Model	Airplane
Wing:		
Area, sq ft . . . . .	3.174	495.94
Span, ft . . . . .	3.095	38.69
Aspect ratio . . . . .	3.014	3.014
Mean geometric chord, ft . . . . .	1.046	13.075
Incidence, deg . . . . .	0	0
Dihedral, deg . . . . .	0	0
Sweepback (at 0.25c line), deg . . . . .	35	35
Taper ratio . . . . .	0.6	0.6
Airfoil (perpendicular to 0.25c line) . .	Symmetrical	Symmetrical
Maximum thickness, percent c . . . . .	12	12
Location of maximum thickness, percent c . .	40	40
Vertical tail:		
Area (two), sq ft . . . . .	0.82	128.125
Aspect ratio . . . . .	1.75	1.75
C.G. location, percent M.G.C. . . . .	17	15 to 18

~~CONFIDENTIAL~~

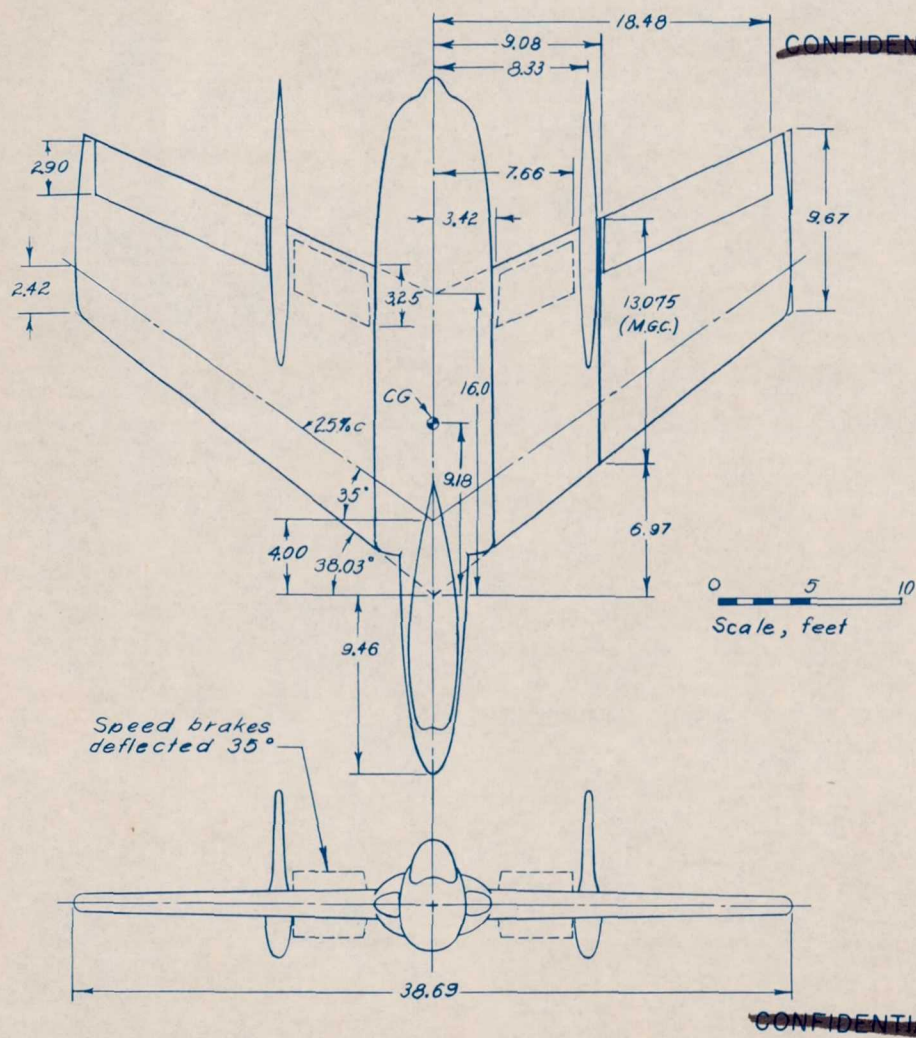


View A-A

~~CONFIDENTIAL~~



Figure 1.- System of axes and control-surface deflections. Positive values of forces, moments, and angles are indicated by arrows.



TABULATED DATA

Wing	
Area	495.94 sq ft
Aspect ratio	3.014
Mean geometric chord	13.08 ft
Incidence	0°
Dihedral	0°
Airfoil (perpendicular to 0.25c)	Symmetrical
Max. thickness	0.12c
Location of max. thickness	0.40c
Vertical tail	
Area (two)	128.13 sq ft
Aspect ratio	1.75
CG location	0.17 M.G.C.

Figure 2.- General arrangement of the Chance Vought XF7U-1 airplane.

~~CONFIDENTIAL~~

NACA RM No. SL8115



Figure 3.- Photograph of the 0.08-scale model of the XF7U-1 airplane mounted on the center sting at a positive angle of attack.

~~CONFIDENTIAL~~

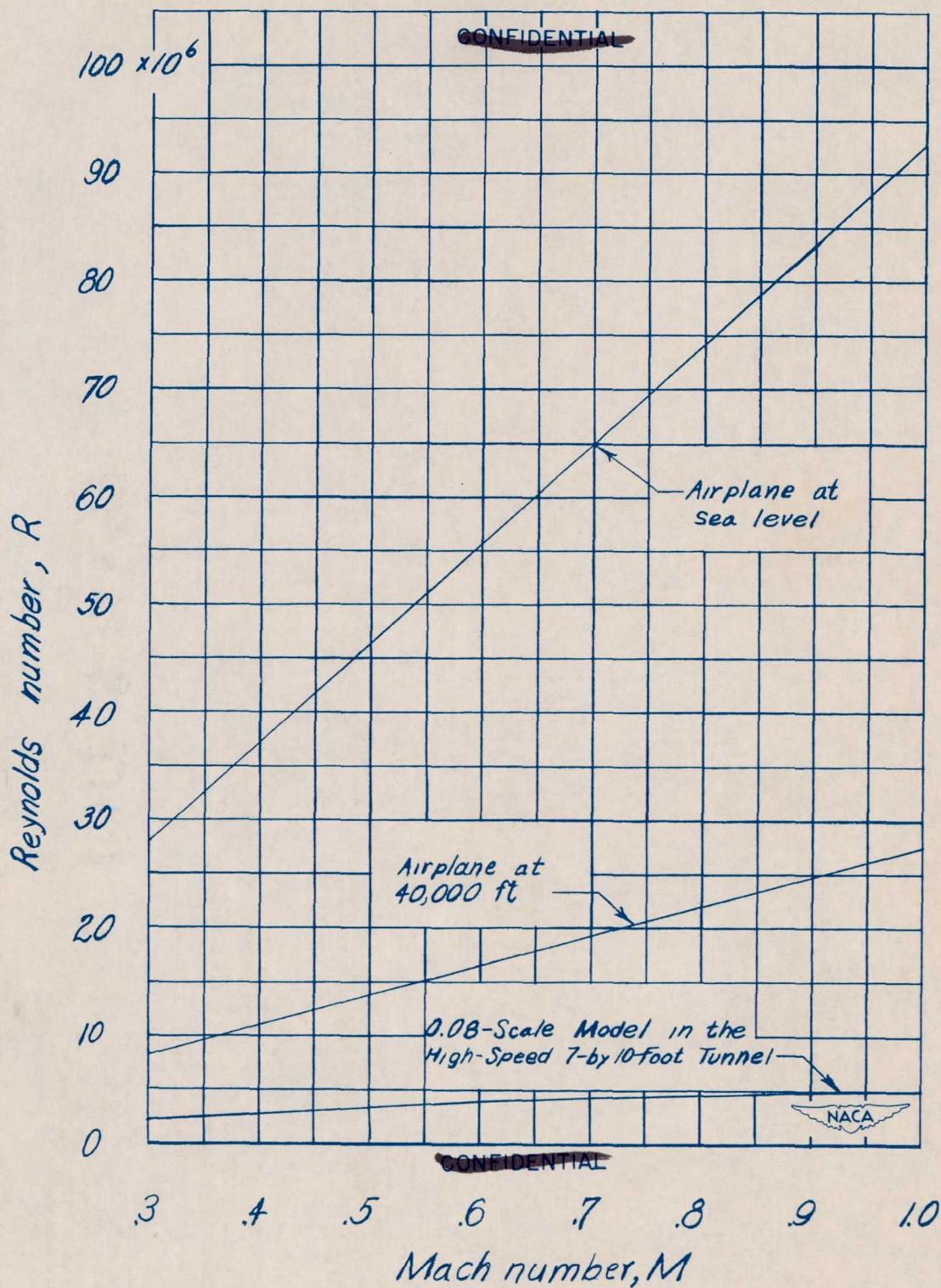


Figure 4.- Variation of Reynolds number with Mach number for flight of the XF7U-1 airplane at two altitudes and for wind-tunnel test data.

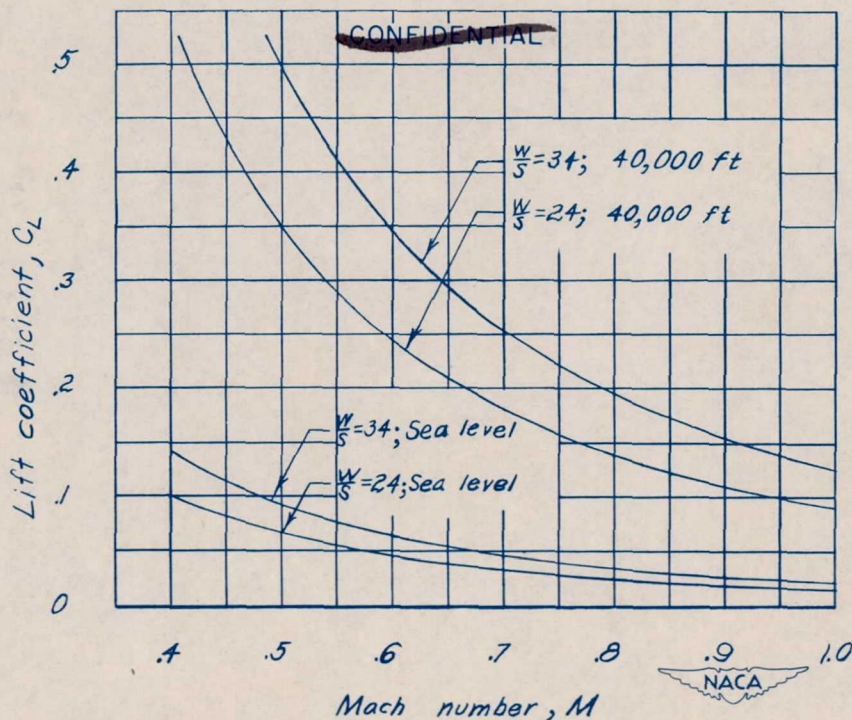


Figure 5.- Variation with Mach number of the lift coefficient required for level flight at various altitudes and wing loadings.

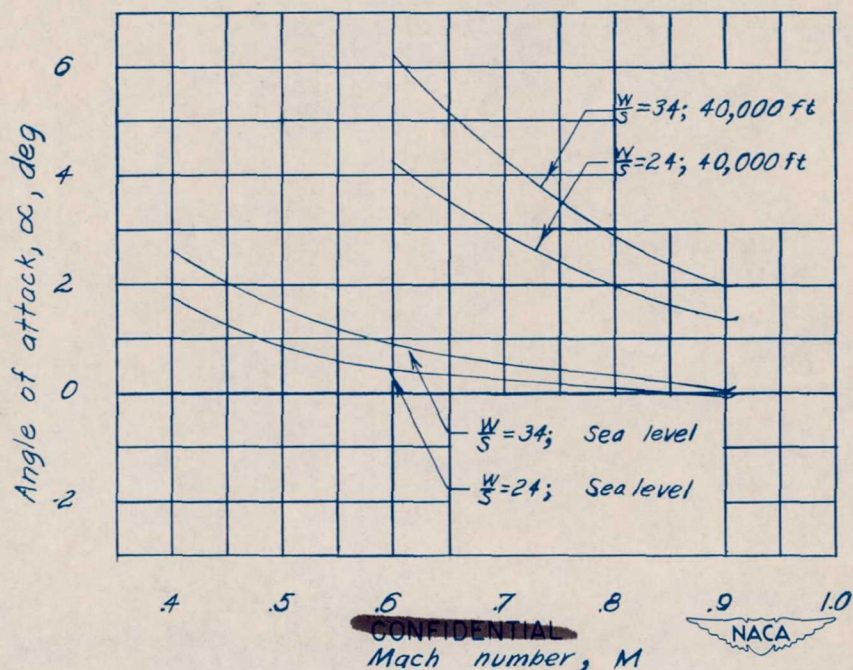


Figure 6.- Variation with Mach number of the angle of attack required for level flight at various altitudes and wing loadings.

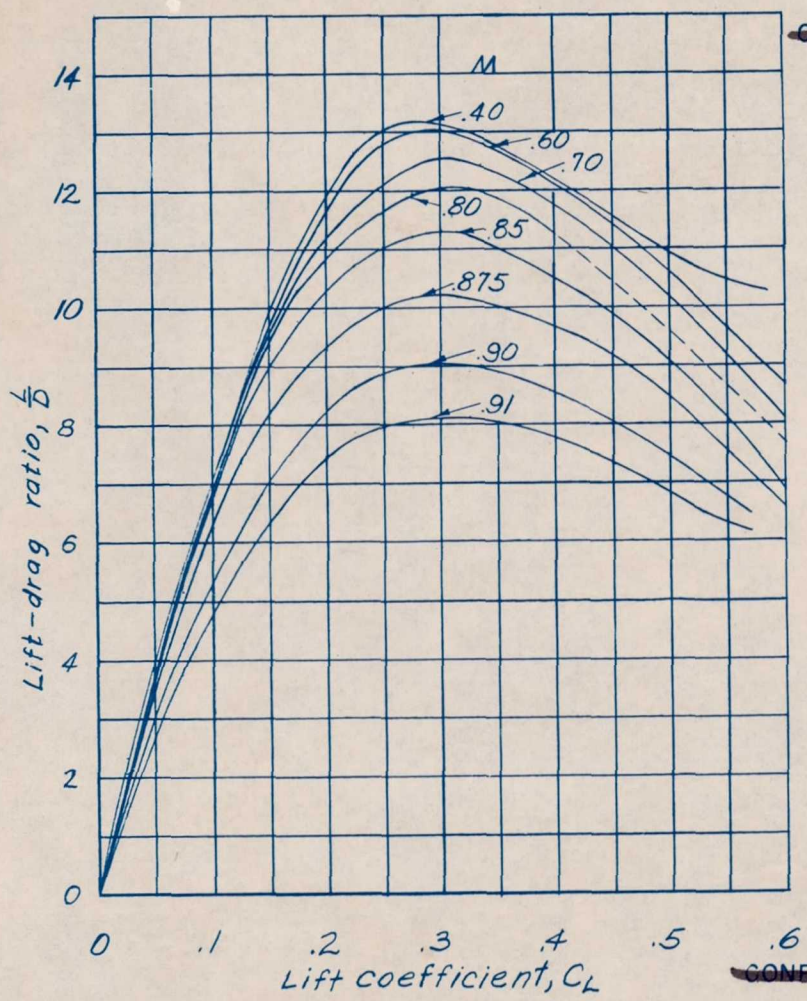


Figure 7.- Variation with lift coefficient of the lift-drag ratio at various Mach numbers.  $\delta_a = 0^\circ$ .

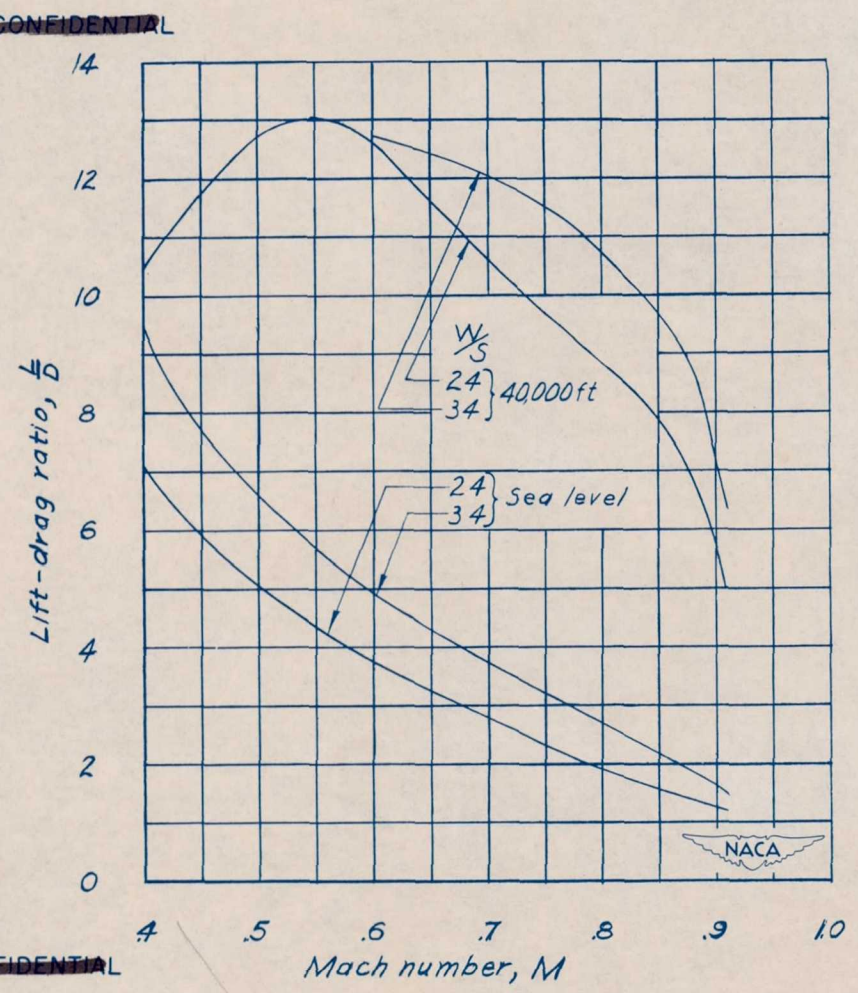


Figure 8.- Variation with Mach number of the lift-drag ratio in level flight at various altitudes and wing loadings. (Trimmed.)

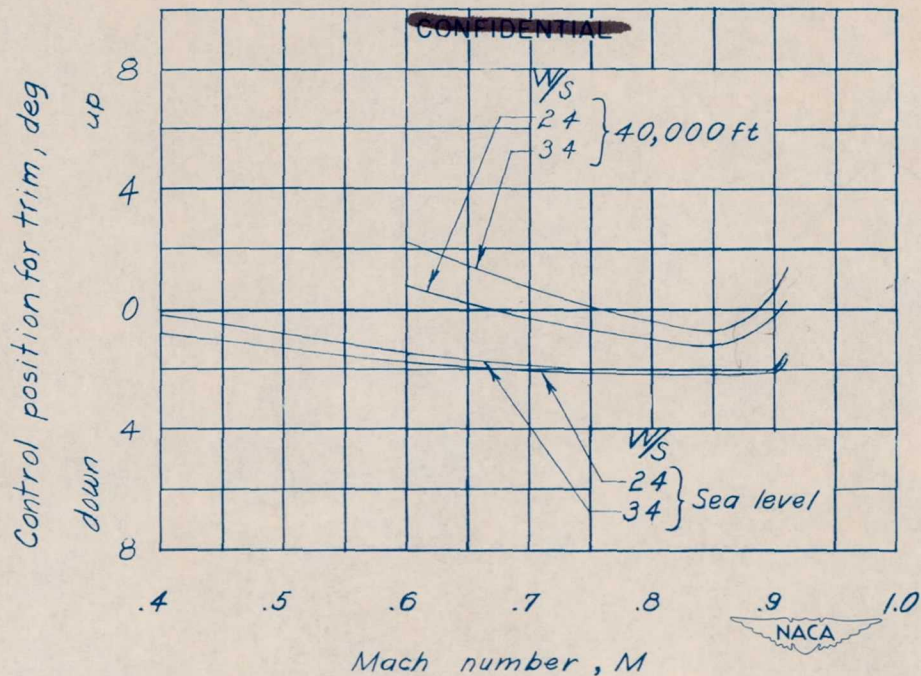


Figure 9.- Variation with Mach number of the control position required for trim in level flight at various altitudes and wing loadings.

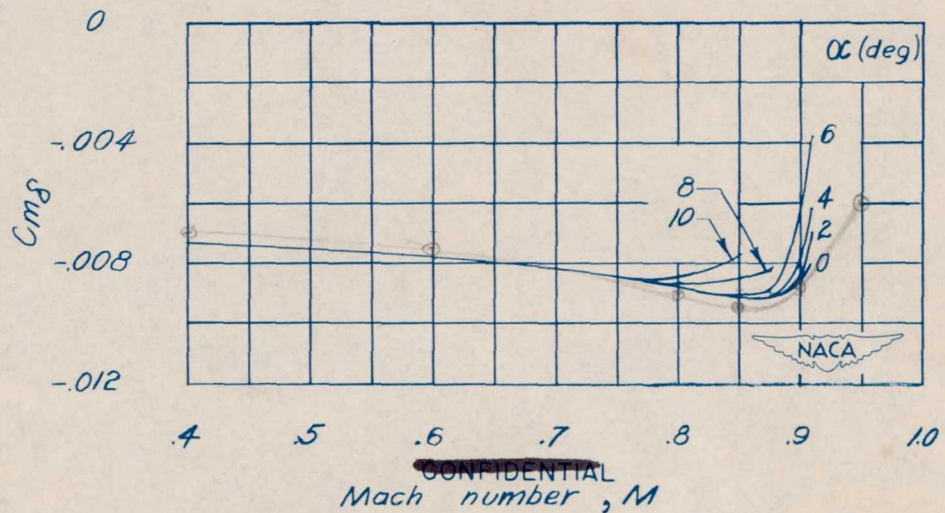


Figure 10.- Variation of the control-effectiveness parameter  $C_{m\delta}$  with Mach number for several angles of attack.

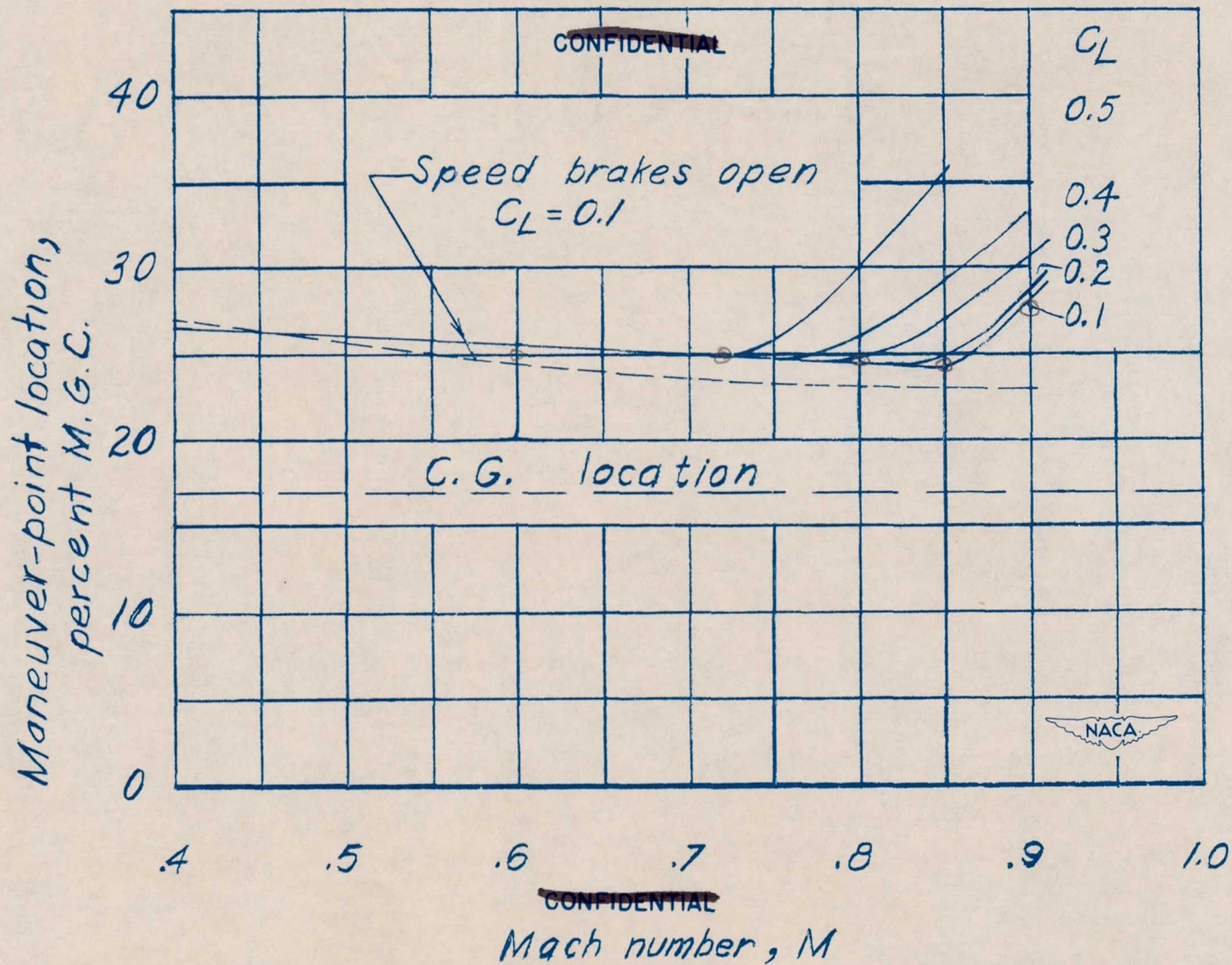
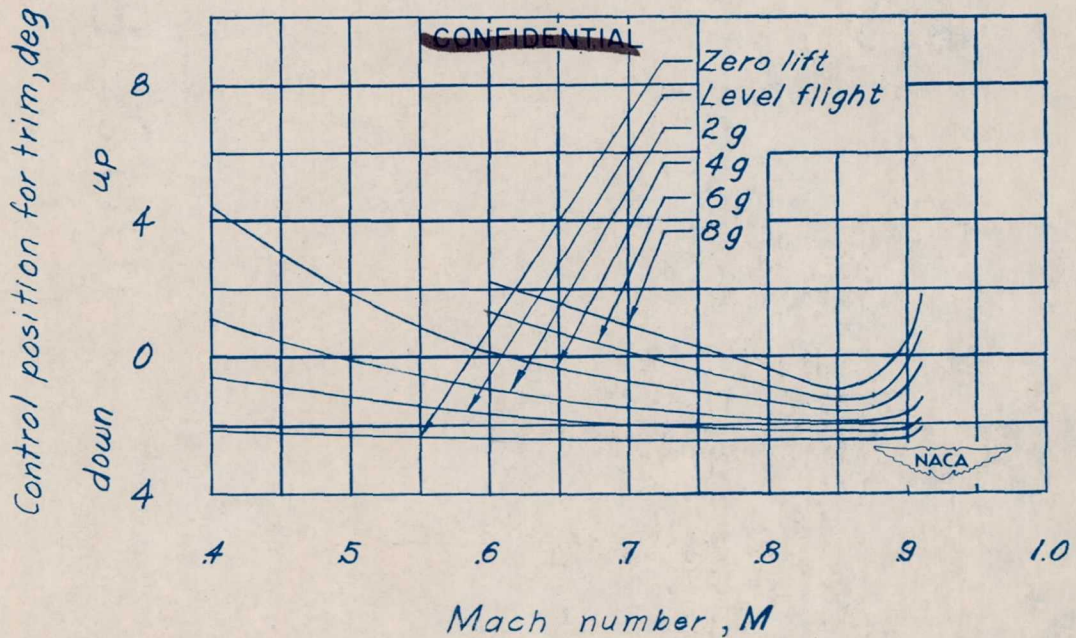
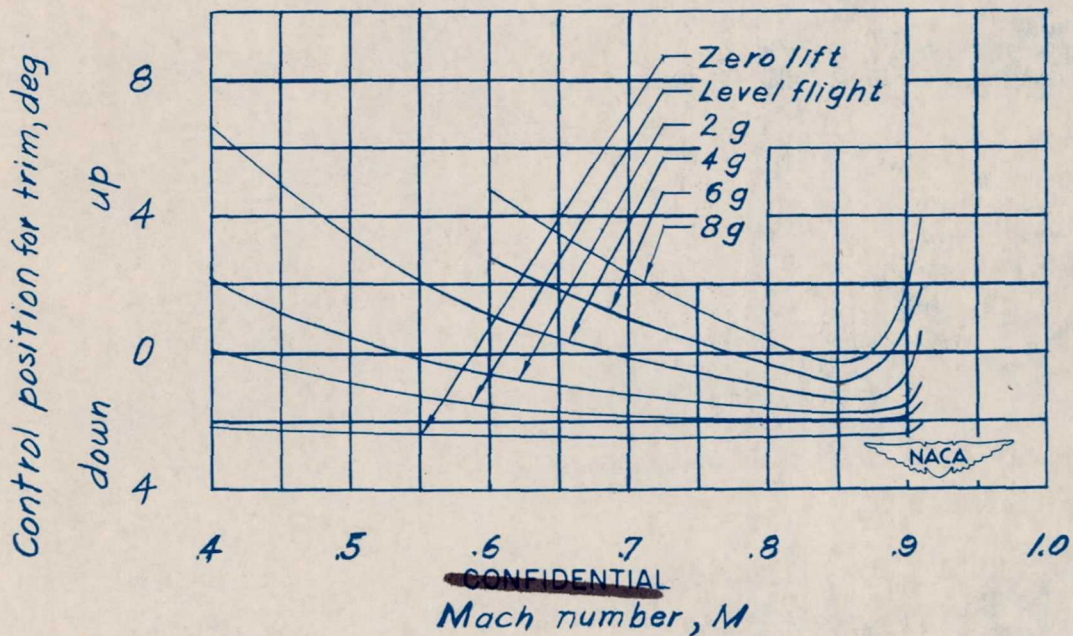


Figure 11.- Variation with Mach number of the maneuver-point location.

23  
25



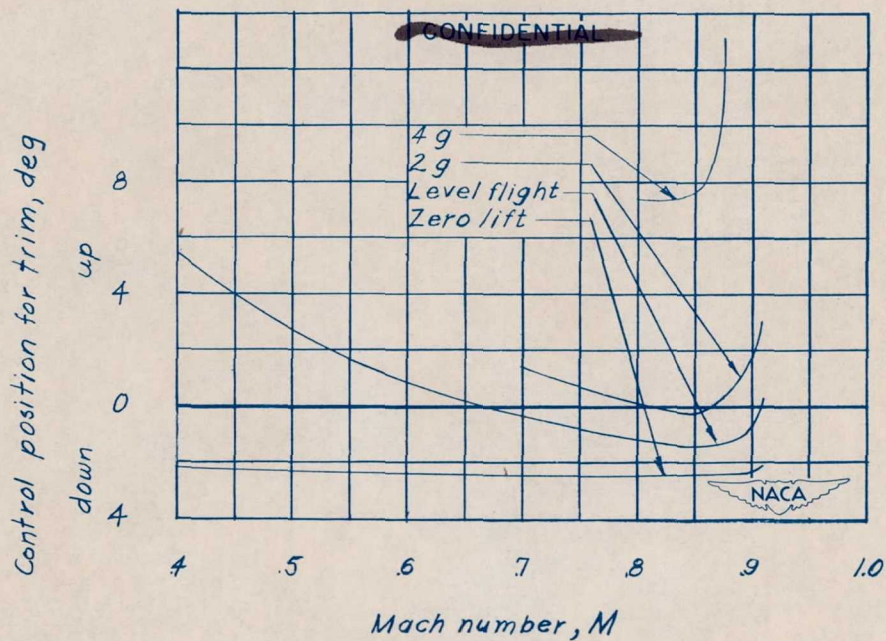
(a) Wing loading of 24.



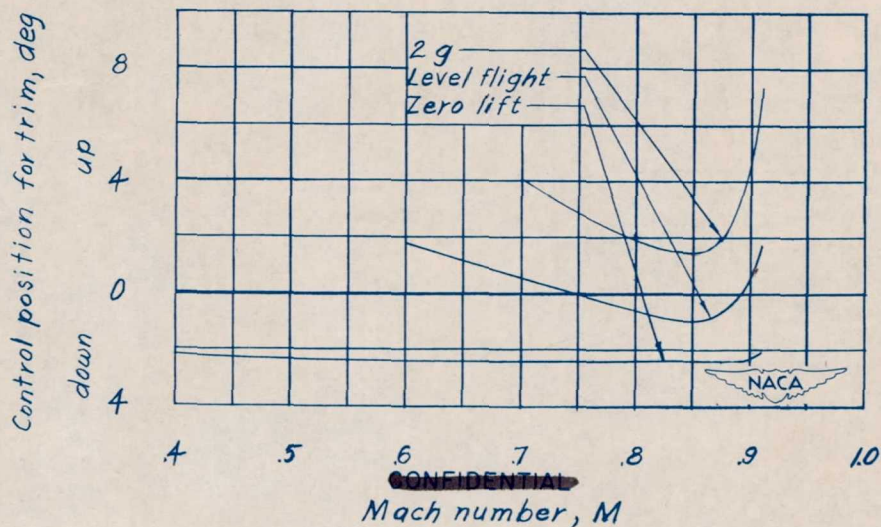
(b) Wing loading of 34.

Figure 12.- Variation with Mach number of the control position required for trim at zero lift, in level, and 2g, 4g, 6g, and 8g accelerated flight at sea level.

205119



(c) Wing loading of 24.



(d) Wing loading of 34.

Figure 12.- Variation with Mach number of the control position required for trim at zero lift, in level and accelerated flight at altitude of 40,000 feet.

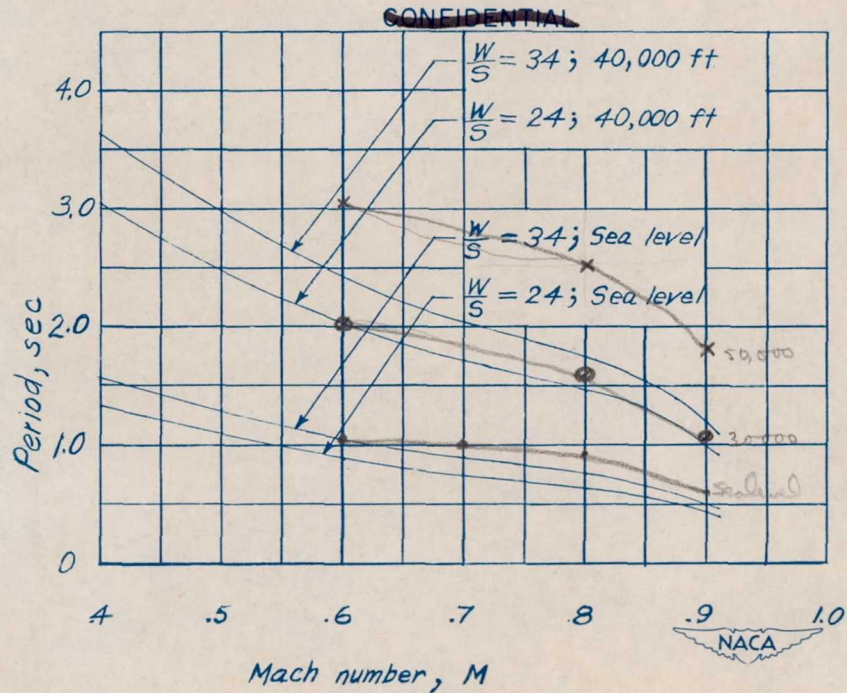


Figure 13.- Variation with Mach number of the period of the short-period longitudinal oscillation.

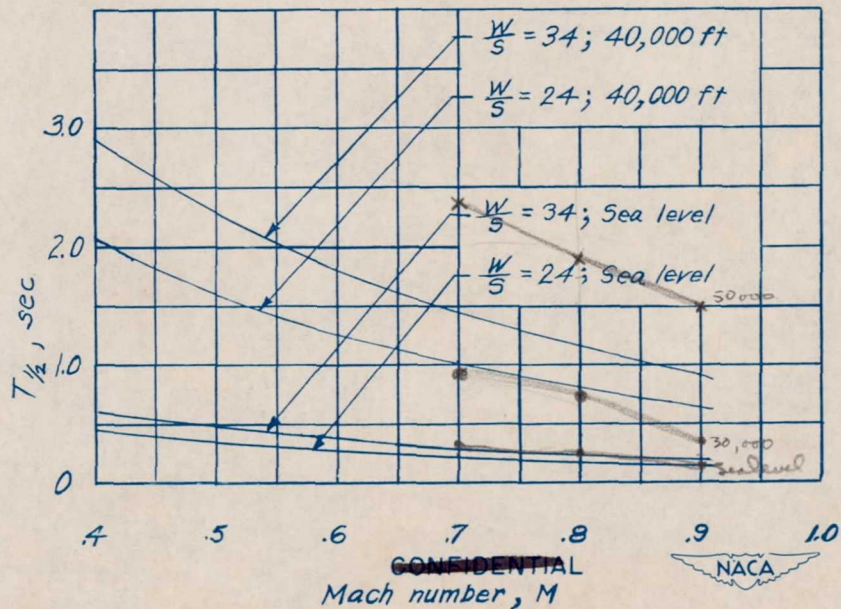


Figure 14.- Variation with Mach number of the time required for the short-period longitudinal oscillation to damp to one-half amplitude.

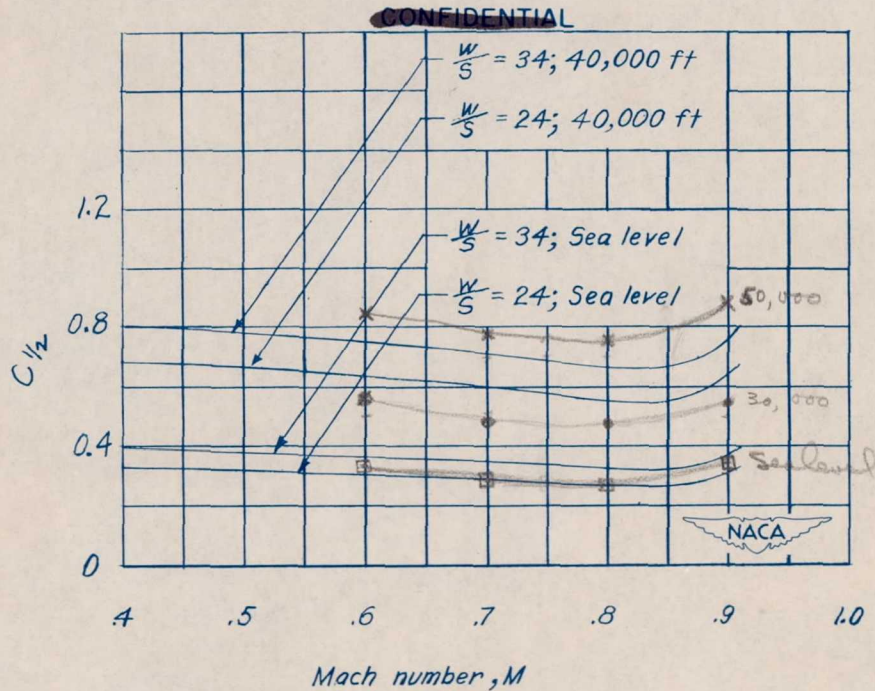


Figure 15.- Variation with Mach number of the number of cycles required for the short-period longitudinal oscillation to damp to one-half amplitude.

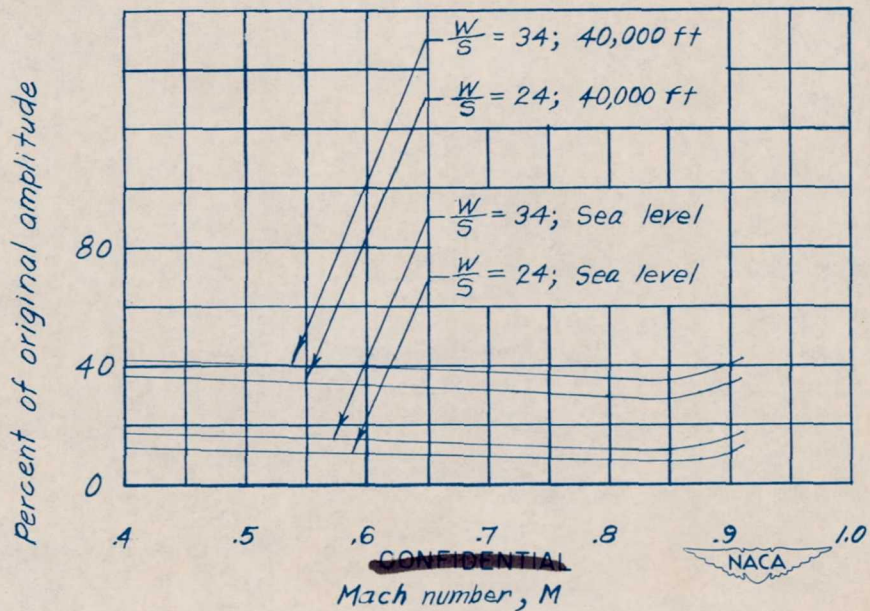


Figure 16.- Variation with Mach number of the amplitude of the short-period longitudinal oscillation after one cycle in percent of the original amplitude.

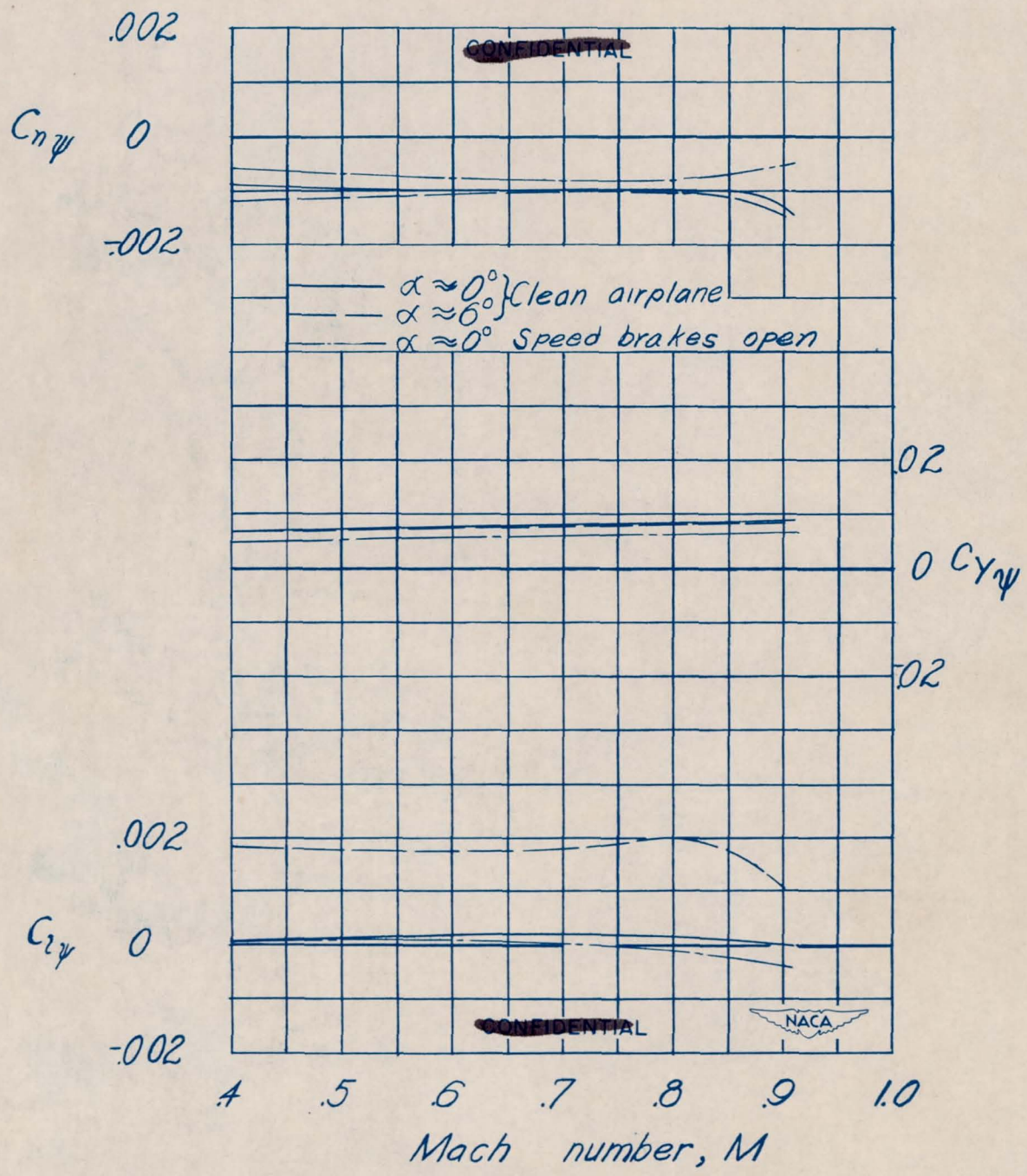


Figure 17.- Variation with Mach number of the lateral stability characteristics of the 0.08-scale model of the Chance Vought XF7U-1 airplane.

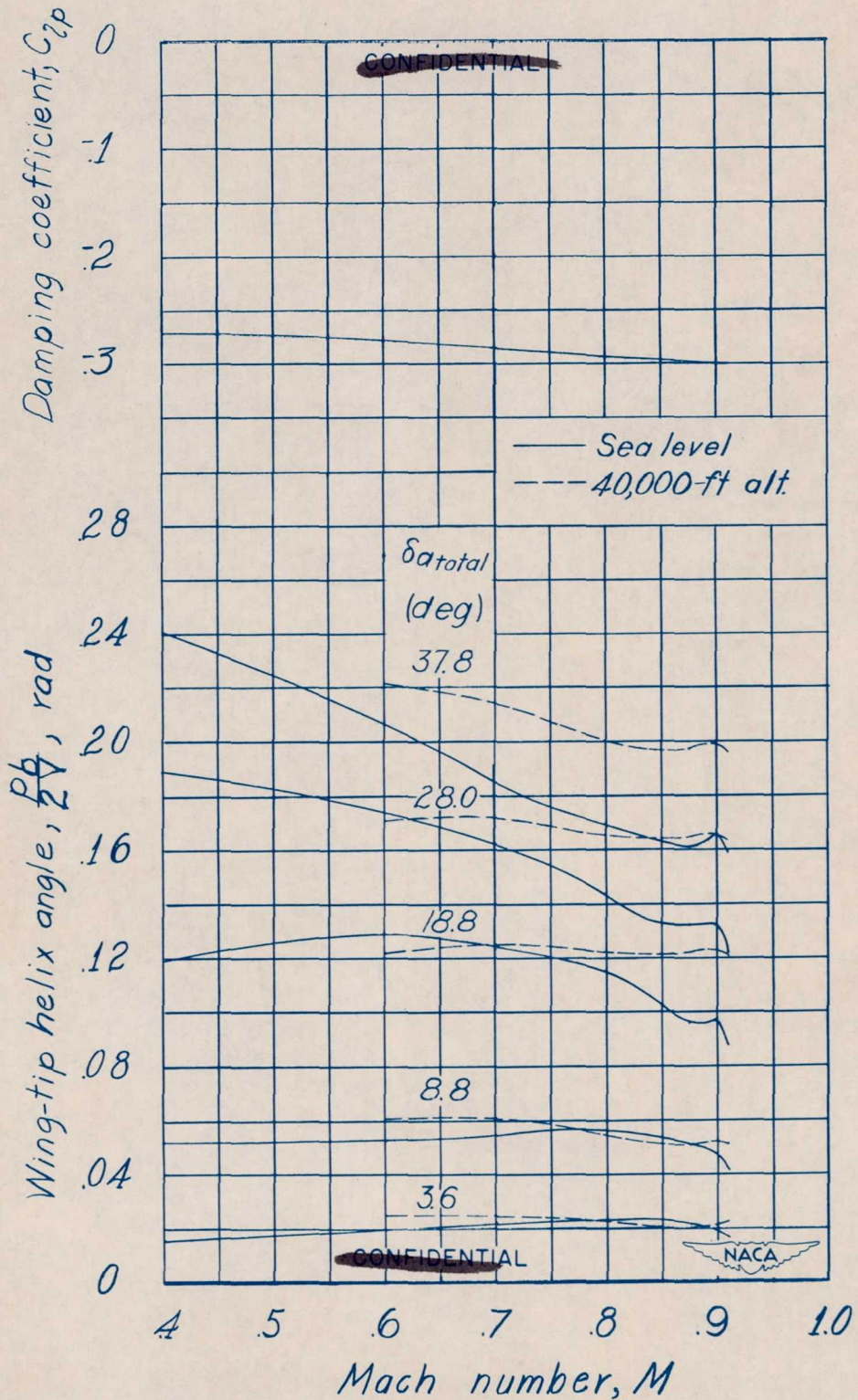


Figure 18.- Variation of the wing-tip helix angle with Mach number for various total aileron deflections.

~~CONFIDENTIAL~~

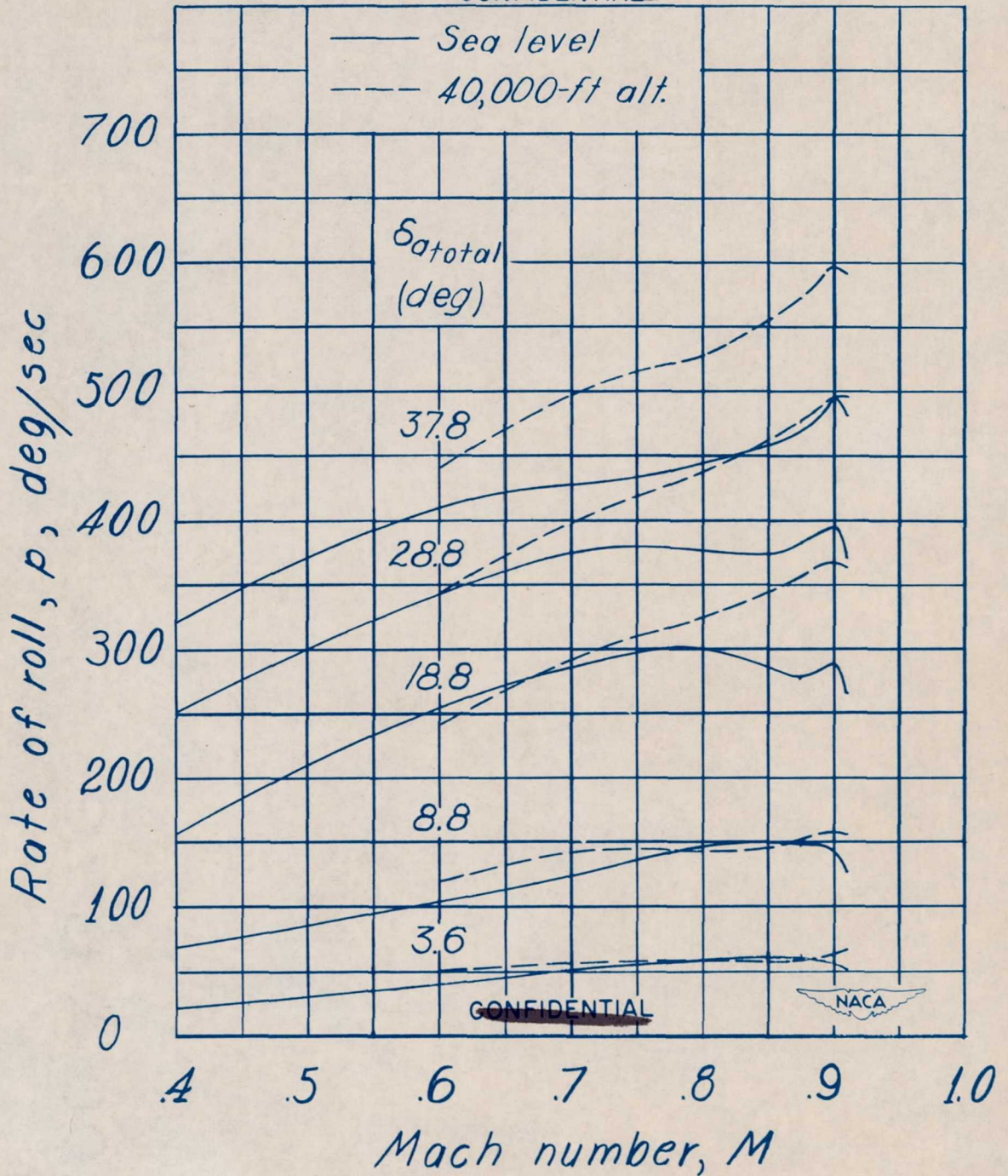


Figure 19.- Variation with Mach number of the rate of roll for various total aileron deflections.

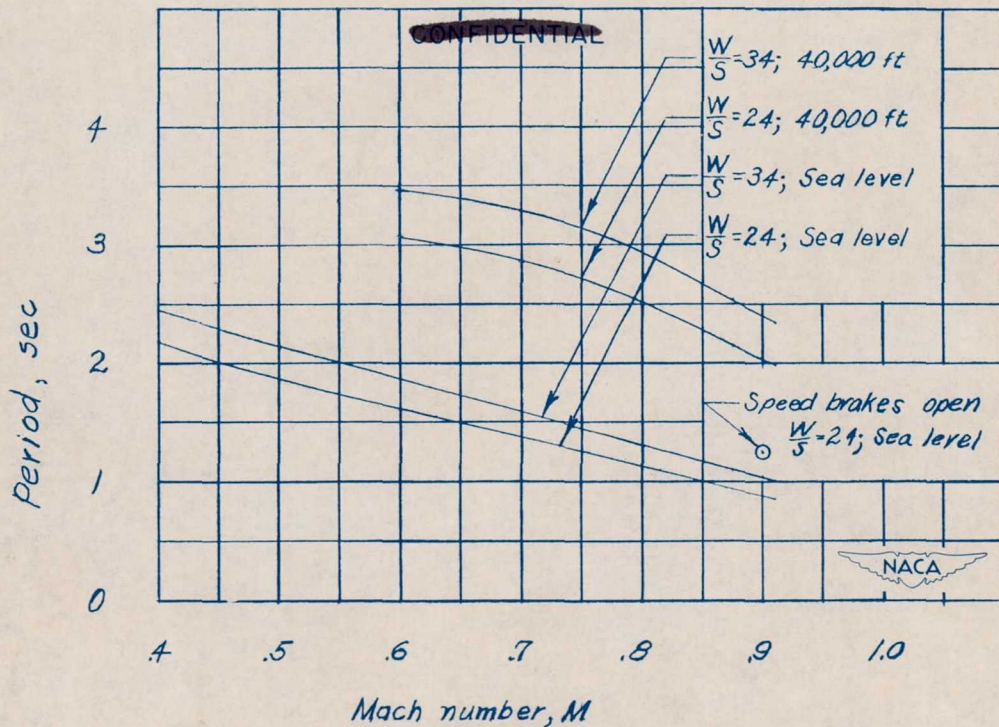
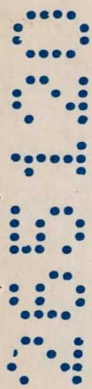


Figure 20.- Variation with Mach number of the period of the lateral oscillation.

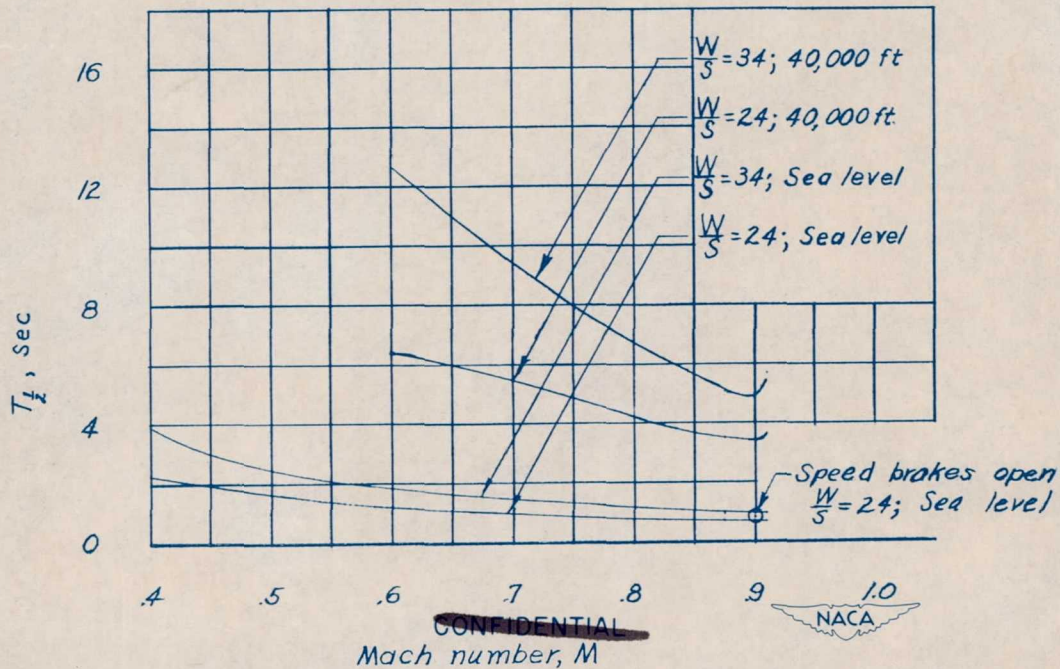


Figure 21.- Variation with Mach number of the time required for the lateral oscillation to damp to one-half amplitude.

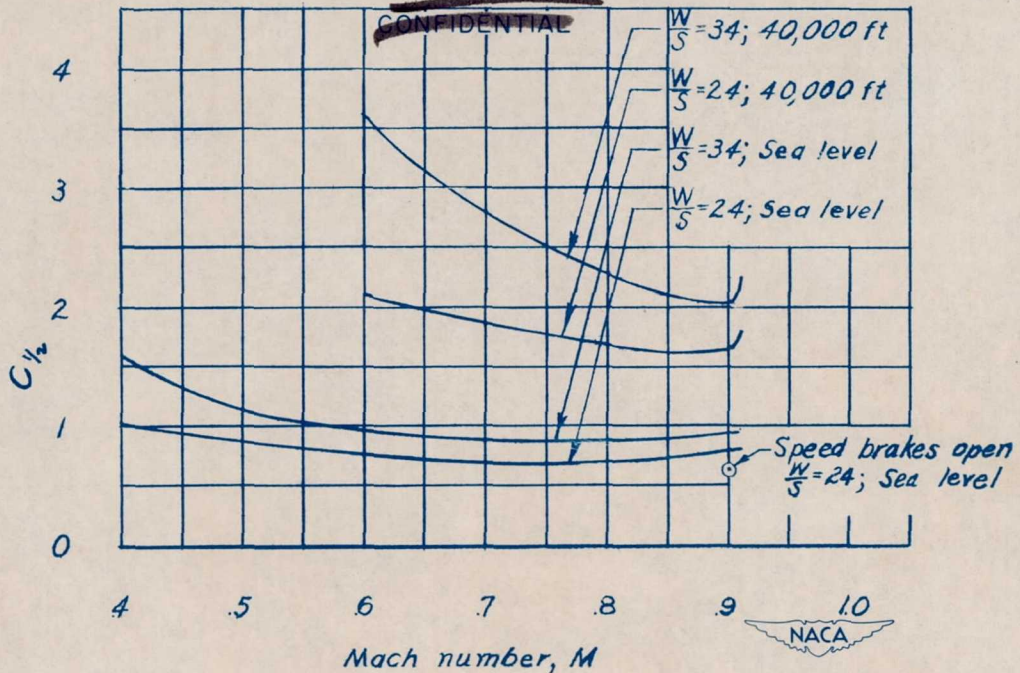


Figure 22.- Variation with Mach number of the number of cycles required for the lateral oscillation to damp to one-half amplitude.

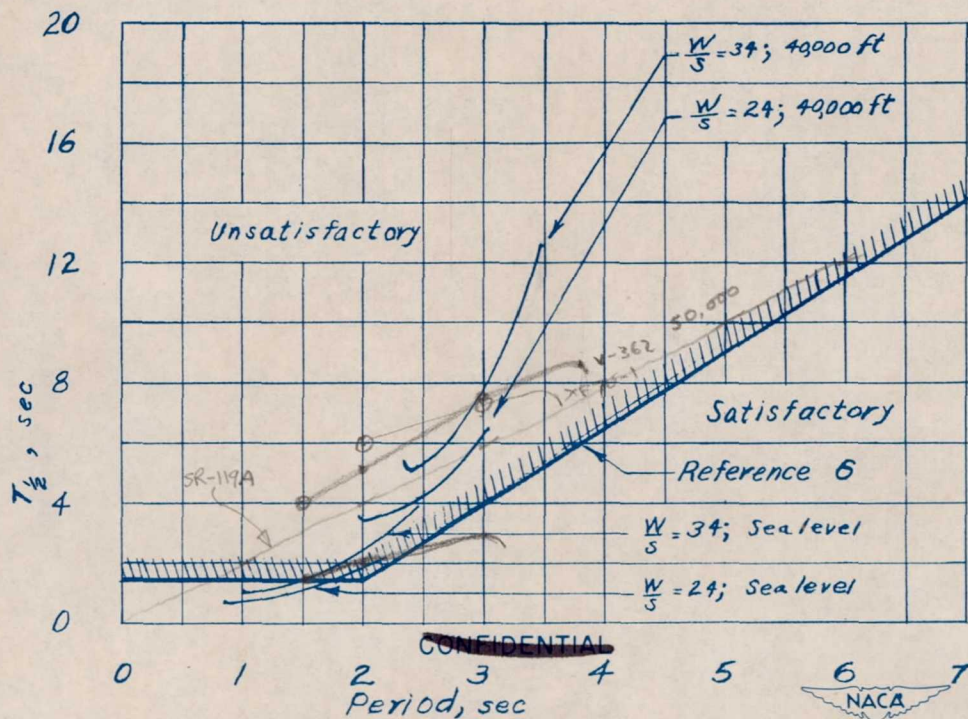


Figure 23.- Variation with period of the time required for the lateral oscillation to damp to one-half amplitude.